Full Length Research Paper

Synthesis and characterization of cubic yttria-stabilized zirconia (8YSZ) nanoparticles by a modified sol-gel route using sucrose and pectin as organic precursors

M. M. Kashani-Motlagh[1]*, A. Maghsoudipour[2], L. Majidzadeh Gorjani[1] and F. Hashemzadeh[1]

[1]Department of Chemistry, Iran University of Science and Technology, Tehran, Iran.
[2]Material and Energy Research Center, Karaj, Iran.

Yttria-stabilized zirconia (YSZ) nanoparticles were synthesized through a sol-gel method using sucrose and pectin as organic precursors. These precursors are abundant in nature and cost effective. Different molar ratio of organic to inorganic (S:Zr^{4+}) precursors were used. To determine the formed phase, x-ray diffraction (XRD) and Raman spectroscopy were performed. XRD pattern showed cubic phase for all S:Zr^{4+} ratios. However, Raman spectroscopy confirmed the cubic phase for samples with higher ratios. Crystallite size of two samples with molar ratio of 1:4 and 1:2 was calculated 17 nm using Scherrer equation. Thermal analysis and IR spectroscopy were applied to determine the reaction pathway.

Key words: Yttria-stabilized zirconia (8YSZ), sol-gel, Raman spectroscopy, cubic phase.

INTRODUCTION

Yttrium-stabilized zirconia, namely: YSZ, is one the most important ceramic oxygen ion conducting materials. It has found great applications as anode and electrolyte of solid oxide fuel cells (SOFC), in oxygen gas sensors and oxygen pumps. Zirconium oxide (ZrO_2) is the most important oxide of zirconia. Four solid phases exist in its pure state: monoclinic, tetragonal, orthorhombic and cubic fluorite structure (Kirk- Othmer, 1998). Zirconium oxide polymorphs transforms as below, although orthorhombic structure has been identified at higher pressure (~10^5 atm) (Yoshimura, 1988):
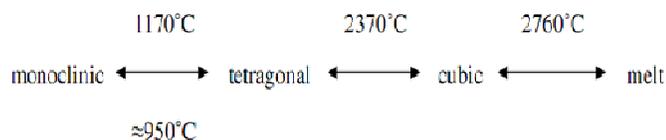
The most stable polymorph is one with the lowest free energy under the specific composition, pressure and temperature. As a consequence, partially stabilized phases, tetragonal and cubic, can be formed at room temperature as tetravalent zirconium ions are replaced by a small amount of Ca^{2+}, Mg^{2+}, Y^{3+}, Yb^{3+}, Gd^{3+}, Sc^{3+} and Nb^{5+} ions (Yoshimura, 1988). Different methods are known to fabricate these solid oxide mixtures as ceramics. Chemical methods have an important place among fabrication processes, and sol-gel is one with great importance to prepare nanoparticles due to advantages associated with it. For example, sol-gel method does not require expensive equipments. On the other hand, there is also increased chemical homogeneity in multi-component systems and high surface area of the gels or powders can be obtained (Suciu et al., 2006, 2008). Studies have shown that in a chemical synthesis through polymer matrix comprising of sucrose (as fuel) and polyvinyl acetate (PVA, as carbonaceous phase) at 200°C without any cationic stabilizer and impurities, the stabilized cubic phase of YSZ is formed. This observation can be attributed to the synthesis method and the resulting crystal size of YSZ (Suciu et al., 2008). In order to obtain nanometer size powders of yttria-stabillized zirconia, several methods of synthesis have been suggested. In most studies, yttria-

---

*Corresponding author. E-mail: m.kashanimotlag@gmail.com.

Table 1. Sucrose to zirconium cation molar ratio (S:Zr^{4+}) in six synthesized samples (1 to 6).

Sample # composition	1	2	3	4	5	6
Sucrose	2	1	1	1	1	2
$ZrCl_4$	100	10	4	2	1	1

Table 2. The steps of temperature program in the calcination process carried out on samples 1 to 6 (Table 1).

Step	Thermal treating
1	1 h up to 200°C
2	1 h kept at 200°C
3	1 h up to 400°C
4	2 h kept at 400°C
5	1.5 h up to 700°C
6	4 h kept at 700°C

stabillzed zirconia has been prepared by solid state reaction at high temperature (>1000°C). In order to reduce synthesis temperature, most of the synthesis methods are based on solution chemistry method such as sol gel (Bachelet et al., 2005; Vlazzi et al., 2006; Kim et al., 2002).

Suciu et al. (2008) have recently reported the use of pectin in the formation of pure cubic phase by sol-gel method. All the analysis data were in consistence with the nanoparticles of a fairly uniform, small size cubic crystal structure and the same quality as is produced using the known organic precursors (Ray et al., 2000; Suciu et al., 2008). Also, Duan et al. (2007) have reported synthesis of cubic and tetragonal zirconia through sol-gel method by changing the precipitants which is another report demonstrating the dependence of structure to the synthesis method (Duan et al., 2007). Rashad and Baioumy have used three processing routes (CP, CGC and MRP) at different thermally treated temperatures which resulted into different polymorphic phases and properties of the produced zirconia nanopowders without using any stabilizers (Rashad and Baioumy, 2008). In this research, we attempted to obtain ultra-fine 8YSZ nanopowders through sol- gel method by replacing traditional organic precursors with sucrose and pectin. The described precursors are more cost-effective, safer, and abundant in nature, so that the process would be more rapid and simple.

EXPERIMENTALS

10 g (0.04 mol) of $ZrCl_4$ (Merck 99%) and 2.86 g (7.46 x 10^{-3} mol) of $Y(NO_3)_3.6H_2O$ (Aldrich, 99.9%) were dissolved in 300 ml of deionized water on a hot plate at 90 to 100°C, respectively. All sucrose:pectin mixtures (organic solutions) with mass ratio of 1:0.02

were prepared by dissolving sucrose and pectin in 200 ml of deionized water at 50 to 80°C to obtain clear solutions. 6 samples with different molar ratio of organic:zirconium cation were prepared (Table 1). After homogenization of the organic solution, it was added to the inorganic one drop-wise, with continuous stirring at 110°C. The thermal treatment at 110°C continued about 2 to 3 h until xerogel was formed. The color of the obtained xerogel depends on the amount of the organic content and changed from cream to brown. Then, the obtained xerogel was dried at 110°C for 1 h in an oven. Finally, the dried xerogel was calcined at 700°C to obtain YSZ nanoparticles (Table 2). Phase determination was performed by x-ray diffraction (XPRD, Siemens, D5000) using Cu K_α (λ = 1.543 nm), the diffraction angle (2θ) from 20 to 70° and Scherrer formula. Raman spectroscopy (Algema Thermo Nicolet Dispersive, Nd:YLF) was carried out to check the XRD results about phase characterization. The process pathway was studied by IR spectroscopy (Shimadzu, 8400S) and thermal analysis (TG- DTA, Perkin Elmer, Pyris Diamond).

RESULTS AND DISCUSSION

The X-ray diffraction data for all samples (1 to 6) as illustrated in Figure 1, showed the reflection characteristics of cubic zirconia, based on JSPDS card #30-1468. The XRD spectra were also used to determine crystallite size by Scherrer Formula 1, where κ is a constant, and here takes as unity, λ the wavelength of Cu $K_{\alpha 1}$ taken as 0.1543 nm, β the full width at half maximum (FWHM) in radiant, and 2θ is the angle of the mode of the peak and D is the mean size of the ordered crystalline. On a more point of view, the X-ray determination of particle sizes (Scherrer) leads to coherent diffracting domains size, not to actual grain size, the former is generally much smaller than the sizes deduced from direct observations:

$$D_{hkl} = \kappa \lambda / \beta \cos\theta \qquad (1)$$
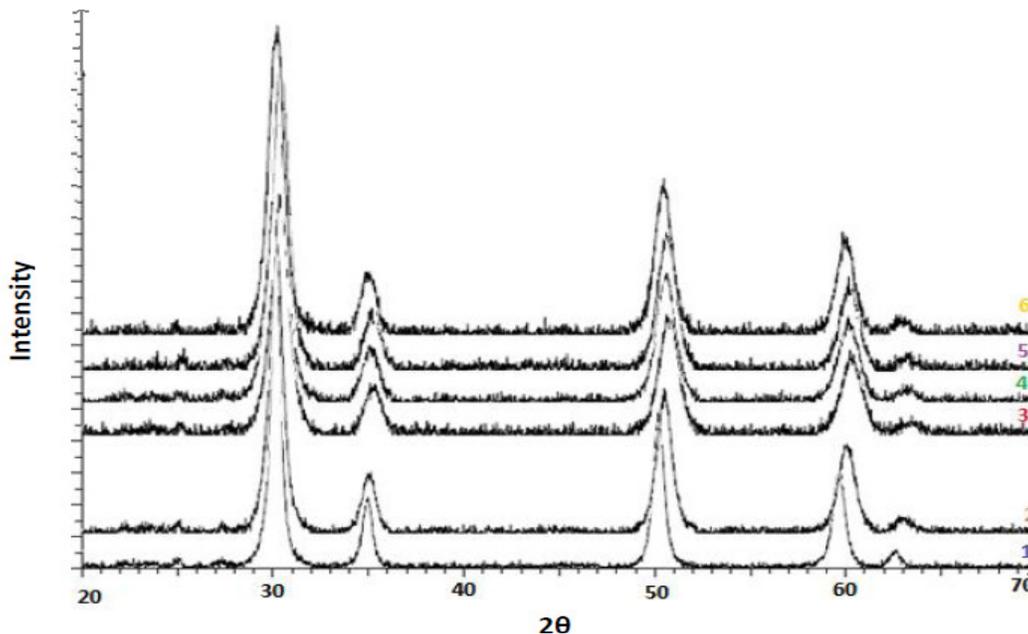
Figure 1. X-ray diffraction patterns of samples 1 to 6 in Table 1 at 2θ range between 20 to 70°C. Samples synthesized with molar ratio of S:Zr^{4+}: (1) 2:100;   (2) 1:10;   (3) 1:4;   (4) 1:2;   (5) 1:1 and (6) 2:1.

The crystallite sizes for samples 1 to 6 were found to be 31, 23, 17, 17, 18 and 20 nm, respectively. Particle size of 8YSZ samples using first peak corresponded to (111). It should be noted that the X-ray determination of particle sizes by Scherrer, Hall-Williamson, Warren-Averbach or other methods lead to coherent diffracting domains size rather than actual grain/crystallite size. On the other hand, the former is generally much smaller than the sizes deduced from direct observations by TEM or SEM techniques. Samples 3 and 4 had the smallest size. These results can be attributed to the use of sufficient amount of pectin which traps the cations and existence of the sucrose to form a carboxylic acid as chelating agent which helps forming of the fine particles (Suciu et al., 2008; Wu et al., 2004). To confirm the cubic phase formation in samples, two experiments can be performed. 1) A low speed scan X-ray diffraction in the 2θ range between 72 to 75° (single peak around 73° is the specific peak for cubic phase and doublet peak shows the tetragonal phase); 2) Raman spectroscopy (Yoshimura, 1988; Dhas and Patil, 1992). For this purpose, Raman spectroscopy was performed. Cubic to tetragonal phase transition in doped zirconia occurs by both enlargement of one of the crystallographic axes and distortion of oxygen from the ideal position in fluorite structure.

On the other hand, the small atomic scattering factor of oxygen makes it difficult to distinguish between cubic and tetragonal phases near the phase boundary (8 to 10% mol Y_2O_3) by XRD. However, Raman spectroscopy is sensitive to polarizability of oxygen ions and therefore

can be used to detect the symmetry of YSZ (Chervin, 2005). A low speed scan XRD in the 2θ range between 72 to 75° of sample 4 is shown in Figure 2. Presence of a single peak around 73° shows the cubic phase. The Raman spectrum of the Samples 1 and 4 are shown in Figure 3. In Figure 3a, the doublet band observed between 270 to 290 cm^{-1}, the band around 550 cm^{-1}, and presence of a shoulder for the band noted 616 cm^{-1} are relatively distinct bands associated with the tetragonal phase. It should be noted that XRD pattern of Sample 1 shows cubic phase, however the Raman spectroscopy does not confirm the XRD result. From these results we can conclude that crystallographic phase of Sample 1 is tetragonal. It is difficult to distinguish between cubic and tetragonal phases near the phase boundary (8 to 10% mol Y_2O_3) by XRD. However, Raman spectroscopy is sensitive to polarizability of oxygen ions and therefore can be used to detect the symmetry of YSZ. Raman spectrum for sample 4 is shown in Figure 3b. The band at 603 cm^{-1} is the specific one for the cubic structure. The dominant band near 598 to 617 cm^{-1} is assigned to triply degenerate F_2g mode associated with pairs of oxygen atoms in 8YSZ crystal lattice, moving out of phase with one another (Pomfret et al., 2005; Zyuzin et al., 2006; Lee et al., 2001; Ghosh et al., 2006). However, the lack of long range order in the anion sublattice due to oxygen vacancies breaks the selection rules giving rise to several weaker features in the range of 0 to 800 cm^{-1} (Mori et al., 2003). This result is in accordance with the Chervin et al. (2005) report which cubic 8YSZ nanoparticles
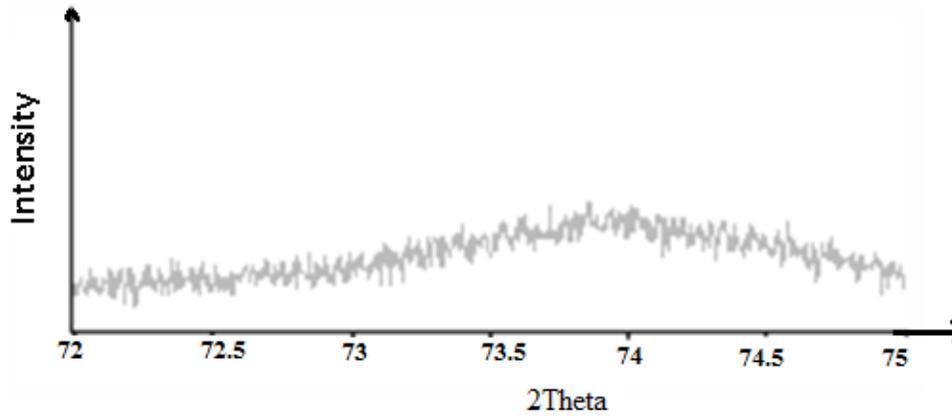
Figure 2. A low scan XRD in the range between 72 to 75°C of Sample 4 (S:Zr^{4+} = 1:2).
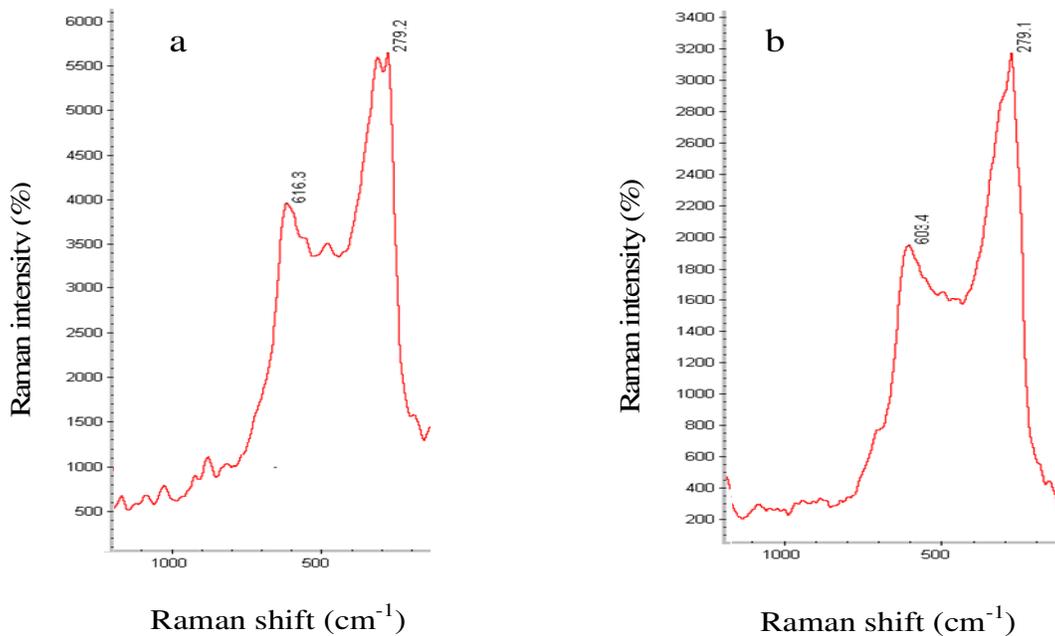
Figure 3. Raman spectrum of the Samples 1(a) (S:Zr^{4+}= 2:100) and (b) 4 (S:Zr^{4+} = 1:2).

synthesized by sol-gel method and calcined at 550°C showed a broad peak between 575 to 640 cm^{-1} having a maximum at 620 cm^{-1} (Chervin et al., 2005). Li et al. (2007) have reported strong peaks at 625 cm^{-1} with additional peaks features at 789, 350, 150 and 40 cm^{-1} which indicates 8YSZ has a cubic structure (Pomfret et al., 2005). Similar results have been reported by Lakki et al. (2000) and Li et al. (2000). However, it was observed that decreasing S/Zr^{4+} molar ratio led to red shift of cubic 8YSZ specific peak position that can be attributed to a larger lattice parameter (Lakki et al., 2000). The thermal analysis was performed for Samples 1 and 4 to trace the

processes taking place during calcination (Figures 4 and 7, respectively).

The weight loss observed in Figure 4 at temperature below 200°C is due to the loss of absorbed moisture (Patil et al., 2008) and/or non-structured water. The weight loss at the temperature range between 200 to 350°C is due to decarboxylation and oxidation reactions of organic compounds (Chervin et al., 2005; Ghosh et al., organic compounds in the polyhydroxyl carboxylic acids structure. At the second experiment, Sample 1 was calcined up to 500°C, kept at this temperature for 5 min and then quenched to remove some amount of organic
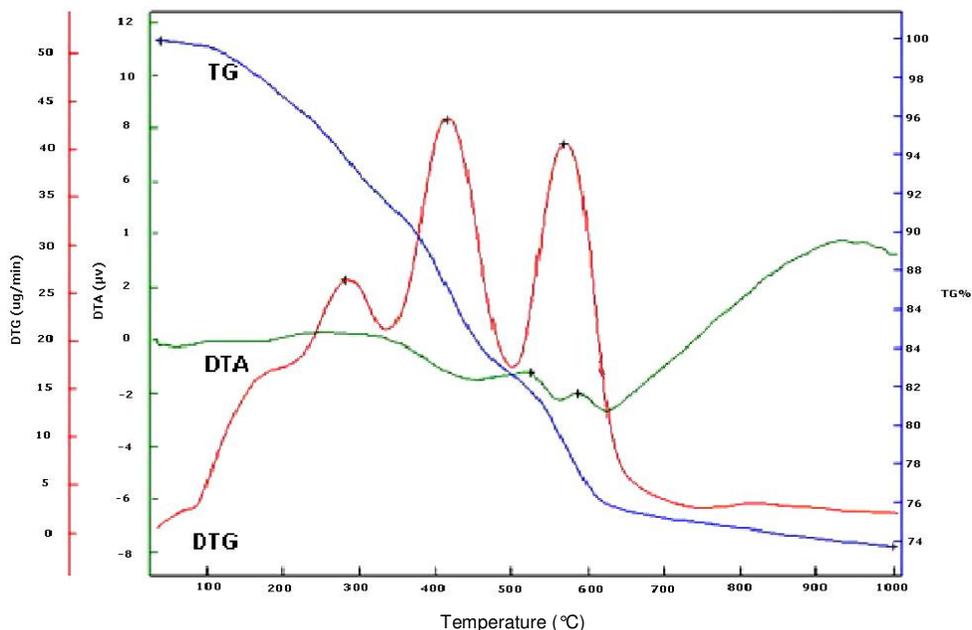
Figure 4. Thermal analysis of Sample 1 (S:Zr^{4+} = 2:100), temperature increased 10°C/min through the air.
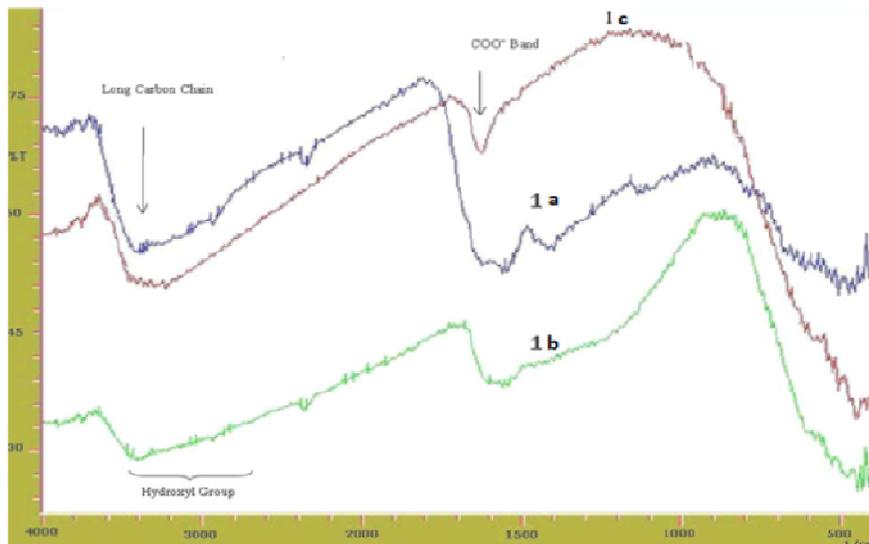
Figure 5. IR spectrum of samples 1a (calcined at 330°C), 1b (calcined at 450°C) and 1c (calcined at 550°C).

2006). The weight loss about 20%, with two maximums at 415 and 569°C can be attributed to the formation and removal of oxidation products (Ray et al., 2000; Suciu et al., 2008). None of the peaks were similar to the one when sucrose was the only compound used as the organic precursor (Prabhakaran et al., 2007). To confirm the occurred processes, two experiments were performed. Firstly, Sample 1 was sintered up to 330, 450, and 550°C (recognized from limiting temperatures of TG curve) and quenched. These samples were called 1a, b and c, respectively. Then, to investigate the species present at those temperatures, IR spectrum of the samples were prepared (Figure 5). IR spectrum of the later samples (1b and c) showed strong band for
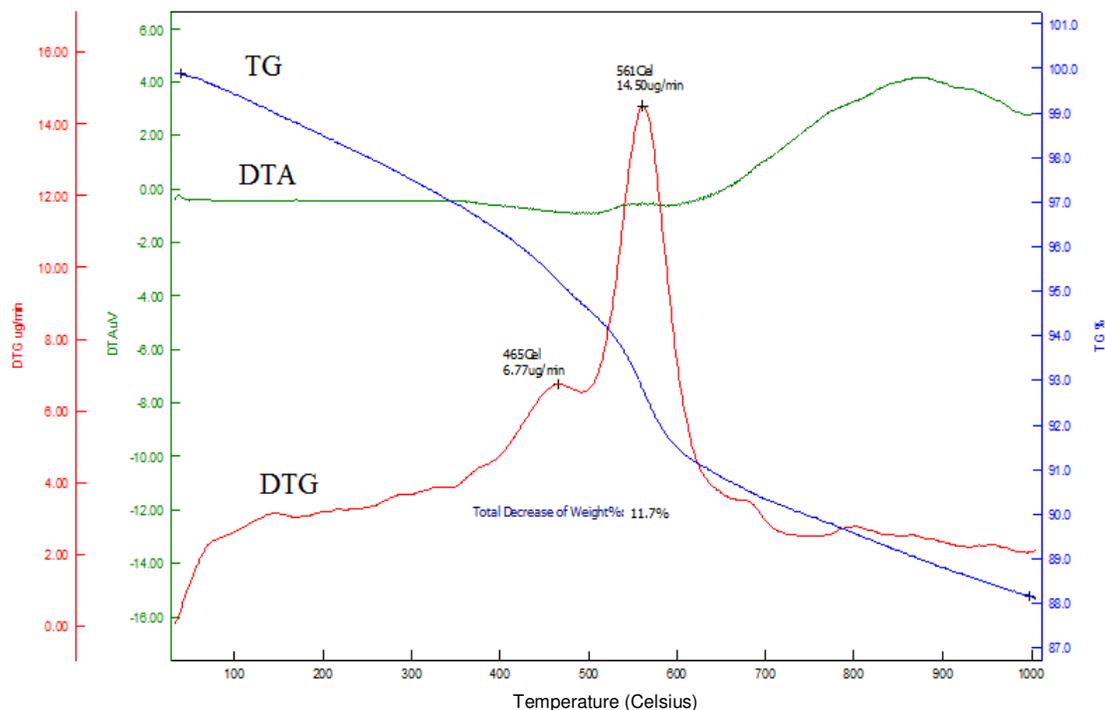
Figure 6. Thermal analysis of Sample 1d (calcined up to 500°C and quenched after 5 min), temperature increased 10°C/min through the air.

carboxylate elimination which continues between 300 to 550°C. Decreasing the intensity of the bands between 2800 to 3600 cm^{-1} may be attributed to the oxidation/removal of the hydroxyl groups and long chain compounds (Sample 1d). The thermal analysis was performed on the obtained sample (Figure 6). Comparing the thermal analysis of Sample 1 with 1d demonstrated that two groups of compounds including organic compounds containing long chain and hydroxyl groups moieties eliminate, respectively. These findings are in accordance with weight loss around 560 to 570°C. However, crystallization peak could not be observed yet (Kuo et al., 2008, 2005). Thermal analysis curve was also obtained for Sample 4 (Figure 7). The first peak is an endothermic one at 112°C which can be attributed to the loss of water. The second and third peaks at 356 and 508°C may be due to oxidation and elimination of organic compounds and correspond to two exothermic peaks on DTA curve. The sample 4 was sintered at the same calcination temperatures for Sample 1. The samples obtained after calcinations up to 300, 450 and 550°C were called 4a, b and c, and their IR spectra were studied (Figure 8). The similar results to the Sample 1 were obtained. This means that increasing of the temperature caused carboxyl removal at first and oxidation of hydroxyl and long chain organic compound in the polyhydroxyl carboxylic acid structure subsequently.

In an additional experiment, Sample 4 was calcined up to 500°C and quenched after 5 min. This sample was called 4d. The similar results to the initial sample were obtained (Figure 9).

CONCLUSIONS

8YSZ nanoparticles were synthesized with relative ease and in simple conditions by organic precursors, sucrose and pectin. Using sucrose and pectin is safe and cost effective. Since calcination temperature is low, fine particles can be obtained. The crystallite size of samples was obtained between 17 and 31 nm, using Scherrer equation for the first peak. The smallest sizes were obtained for the samples with S to Zr^{4+} ratio 1:4 and 1:2. XRD patterns were attributed to the cubic phase formation for all samples. Raman spectroscopy and low speed scan x-ray diffraction specified that sample 4 was cubic 8YSZ but Raman spectroscopy does not confirm of XRD result about Sample 1. The sample with lower S to Zr^{4+} ratio (Sample 1) showed the presence of tetragonal phase either that confirms the effective role of organic precursors in cubic phase formation. Thermal analysis demonstrated three specific regions that encounter the weight loss.

Comparing the IR spectra of the samples calcinated at different temperatures shows that the observed peaks are related to the decarboxylation reactions of organic
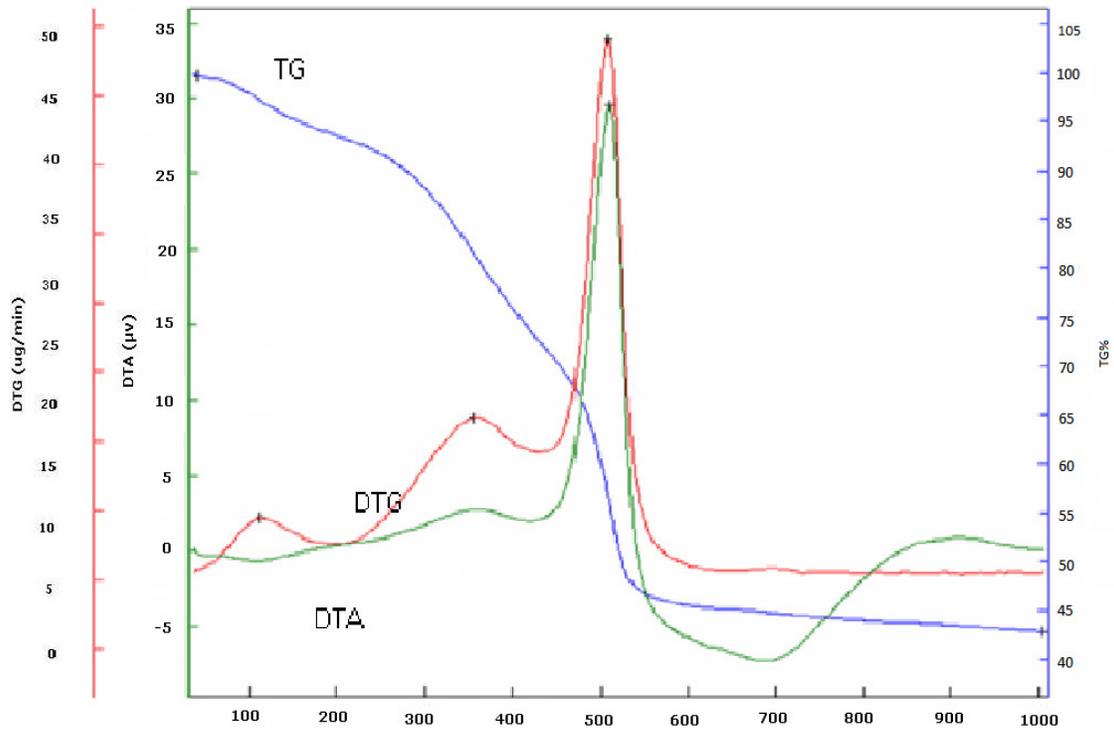
Figure 7. Thermal analysis of Sample 4 (S:Zr^{4+} = 1:2), temperature increased 10°C/min through the air.
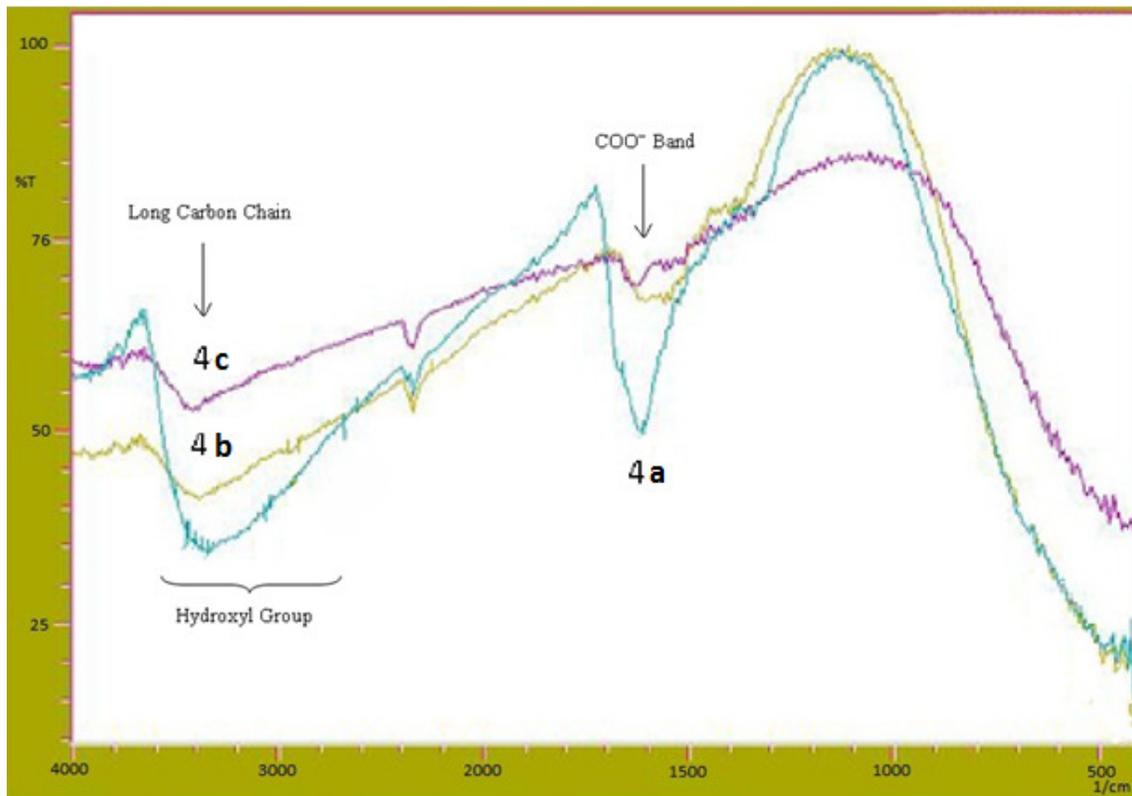
Figure 8. IR spectrum of Samples 4a (calcined at 330°C), 4b (calcined at 450°C) and 4c (calcined at 550°C).
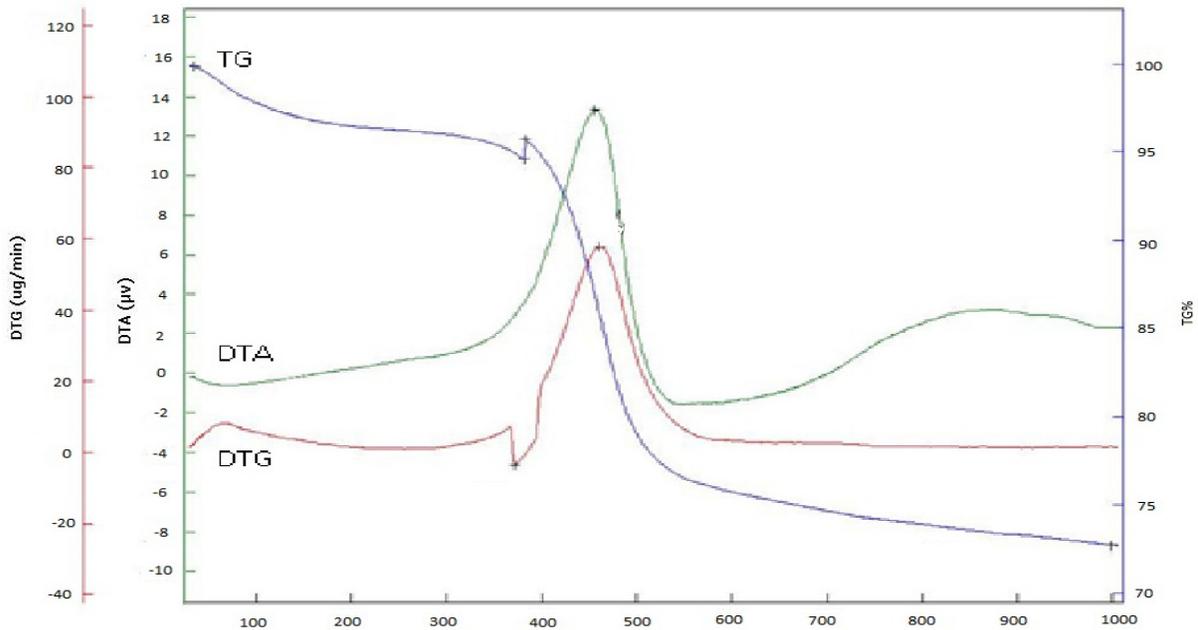
Figure 9. Thermal analysis of Sample 4d (calcined up to 500°C and quenched after 5 min), temperature increased 10°/min through the air.

compounds and hydroxyl and long chain carbon removal.

REFERENCES

Bachelet R, Nahelou G, Boulle A, Guinebretiere R, Dauger A (2005). The belowground view of global models. Prog. Solid State Chem., 33: 327-332.

Chervin CN, Clapsaddle BJ, Chiu HW, Gash AE, Satcher JHJ, Kauzlarich SM (2005). A Non-Alkoxide Sol—Gel Method for the Preparation of Homogeneous. Chem. Mater., 17: 3345.

Dhas NA, Patil KC (1992). Combustion synthesis and properties of NASICON materials. Int. J. Self Propag. High Temp. Synth., 1: 576.

Duan G, Yang X, Lu A, Huang G, Lu L, Wang X (2007). Applications of systems biology. Mater. Charact., 58: 78.

Ghosh A, Suri AK, Pandey M, Thomas S, Rama Mohan TR, Rao BT (2006). Nanocrystalline zirconia-yttria system-a Raman study. Mater. Lett., 60: 1170.

Kim SG, Yoon SP, Nam SW, Hyun SA (2002). View Record in Scopus. Power Sour. J., 110: 222-228.

Kirk- Othmer (1998). Encyclopedia of chemical technology. John Wiley & Sons, NY.

Kuo C, Lee Y, Fung K, Wang M (2005). Effect of YO addition on the phase transition and growth of YSZ nanocrystallites prepared by a sol?gel. J. Non-Cryst. Solids, 351: 304.

Kuo C, Lee Y, Hung I, Wang M, Wen S, Fung K, Shih C (2008). Thermal Stability of Ordered. J. Alloys Compd., 453: 470.

Lakki A, Herzog R, Weller M, Schubert H, Reetz C, Grke O, Kilo M, Borchardt G (2000). Mechanical loss, creep, diffusion and ionic conductivity of ZrO2-8. J. Eur. Ceram. Soc., 20: 285.

Lee DY, Jang J, Kim D (2001). Expressed sequence tags and mRNA. Ceram. Int., 27: 291.

Li Q, Xia T, Liu XD, Ma XF, Meng J, Cao XQ (2007). Fast densification and electrical conductivity of yttria. Mater. Sci. Eng. B., 138: 78.

Mori M, Hiei Y, Itoh H, Tompsett G, Sammes N (2003). Evaluation of Ni and Ti-doped Y2O3 stabilized ZrO2 ... oxide fuel cells. Solid State Ionics, 160: 1.

Patil DS, Prabhakaran K, Dayal R, Prasad CD, Gokhale NM, Samui AB, Sharma SC (2008). A dip coating process. Ceram. Int., 34: 1195.

Pomfret MB, Stoltz C, Varughese B, Walker RA (2005). Structural and compositional characterization of yttria-stabilized zirconia: Anal. Chem., 77: 1791.

Prabhakaran K, Melkeri A, Gokhale NM, Sharma SC (2007). Preparation of a porous cermet SOFC substrate by gelcastin. Ceram. Int., 33: 1551.

Rashad MM, Baioumy HM (2008). Effect of thermal treatment on the crystal structure and morphology of zirconia nanopowders produced by three different routes. J. Mater. Process. Technol., 195: 178.

Ray JC, Pati RK, Pramanik P (2000). A novel chemical route for the synthesis ... yttria stabilized zirconia (YSZ). J. Eur. Ceram. Soc., 20: 1289.

Suciu C, Gagea L, Hoffmann AC, Mocaen M (2006). Evaluation of overshooting errors in particle methods for diffusion by biased global. Chem. Eng. Sci., 61: 7831.

Suciu C, Hoffmann AC, Kosinski P (2008). Obtaining YSZ nanoparticles by the sol-gel method with sucrose and pectin as organic precursors. J. Mater. Process. Technol., 202: 316.

Suciu C, Hoffmann AC, Vik A, Goga F (2008). Effect of calcination conditions and precursor proportions on the properties of YSZ nanoparticles obtained by modified sol-gel route. Chem. Eng. J., 138: 608.

Viazzi C, Deboni A, Ferreira JZ, Bonino JP, Ansart F (2006). Synthesis of yttria. Solid State Sci., 8: 1023-1028.

Vlazzi C, Bonino JP, Ansart F (2006). Fluorescence microscopy for studying the viability of micro-organisms in natural whey starters. Surf. Coat Technol., 201: 3889-3893.

Wu Y, Bandyopadhyay A, Bose S (2004). Processing of alumina and zirconia nano-powders and compacts. Mater. Sci. Eng. A., 380: 349.

Yoshimura M (1988). Phase stability of zirconia. Ceram Bull., 67: 1950.

Zyuzin DA, Cherepanova SV, Moeoz EM, Burgina EB, Sadykov VA, Kostrovskii VG, Matyshak (2006). Mooz-lum reviews and showtimes: Movies on Going Out Guide. J. Solid State Chem., 179: 2965.